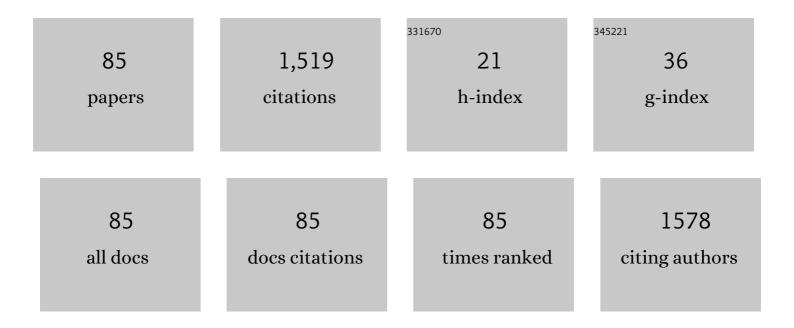
List of Publications by Year in descending order

Source: https://exaly.com/author-pdf/7928376/publications.pdf Version: 2024-02-01



#	Article	IF	CITATIONS
1	A Flexible Temperature Sensor Based on Reduced Graphene Oxide for Robot Skin Used in Internet of Things. Sensors, 2018, 18, 1400.	3.8	180
2	MXene/Polymer Nanocomposites: Preparation, Properties, and Applications. Polymer Reviews, 2021, 61, 80-115.	10.9	123
3	A Harsh Environment-Oriented Wireless Passive Temperature Sensor Realized by LTCC Technology. Sensors, 2014, 14, 4154-4166.	3.8	90
4	A Wireless Passive Pressure and Temperature Sensor via a Dual LC Resonant Circuit in Harsh Environments. Journal of Microelectromechanical Systems, 2017, 26, 351-356.	2.5	57
5	A LC wireless passive temperature-pressure-humidity (TPH) sensor integrated on LTCC ceramic for harsh monitoring. Sensors and Actuators B: Chemical, 2018, 270, 433-442.	7.8	54
6	Diaphragm-Free Fiber-Optic Fabry-Perot Interferometric Gas Pressure Sensor for High Temperature Application. Sensors, 2018, 18, 1011.	3.8	53
7	A Novel Surface <inline-formula> <tex-math notation="LaTeX">\$LC\$ </tex-math> </inline-formula> Wireless Passive Temperature Sensor Applied in Ultra-High Temperature Measurement. IEEE Sensors Journal, 2019, 19, 105-112.	4.7	42
8	Fiber-optic Fabry–Perot pressure sensor based on sapphire direct bonding for high-temperature applications. Applied Optics, 2019, 58, 1662.	1.8	42
9	Review of Research Status and Development Trends of Wireless Passive LC Resonant Sensors for Harsh Environments. Sensors, 2015, 15, 13097-13109.	3.8	40
10	Highly Sensitive NH3 Wireless Sensor Based on Ag-RGO Composite Operated at Room-temperature. Scientific Reports, 2019, 9, 9942.	3.3	40
11	A High-Temperature Piezoresistive Pressure Sensor with an Integrated Signal-Conditioning Circuit. Sensors, 2016, 16, 913.	3.8	38
12	A Novel Metamaterial Inspired High-Temperature Microwave Sensor in Harsh Environments. Sensors, 2018, 18, 2879.	3.8	38
13	A High Temperature Capacitive Pressure Sensor Based on Alumina Ceramic for in Situ Measurement at 600 ŰC. Sensors, 2014, 14, 2417-2430.	3.8	35
14	Fiber-optic Fabry–Perot pressure sensor based on low-temperature co-fired ceramic technology for high-temperature applications. Applied Optics, 2018, 57, 4211.	1.8	35
15	Antenna-resonator integrated wireless passive temperature sensor based on low-temperature co-fired ceramic for harsh environment. Sensors and Actuators A: Physical, 2015, 236, 299-308.	4.1	31
16	Low-Cost Wireless Temperature Measurement: Design, Manufacture, and Testing of a PCB-Based Wireless Passive Temperature Sensor. Sensors, 2018, 18, 532.	3.8	30
17	An Embedded Passive Resonant Sensor Using Frequency Diversity Technology for High-Temperature Wireless Measurement. IEEE Sensors Journal, 2015, 15, 1055-1060.	4.7	27
18	LC temperature-pressure sensor based on HTCC with temperature compensation algorithm for extreme 1100 °C applications. Sensors and Actuators A: Physical, 2018, 280, 437-446.	4.1	26

#	Article	IF	CITATIONS
19	Thermopile Infrared Detector with Detectivity Greater Than 108ÂcmHz(1/2)/W. Journal of Infrared, Millimeter, and Terahertz Waves, 2010, 31, 810-820.	2.2	25
20	Characterization of biomechanical properties of cells through dielectrophoresis-based cell stretching and actin cytoskeleton modeling. BioMedical Engineering OnLine, 2017, 16, 41.	2.7	25
21	An LC Passive Wireless Gas Sensor Based on PANI/CNT Composite. Sensors, 2018, 18, 3022.	3.8	23
22	Dielectrically-Loaded Cylindrical Resonator-Based Wireless Passive High-Temperature Sensor. Sensors, 2016, 16, 2037.	3.8	22
23	Slot Antenna Integrated Re-Entrant Resonator Based Wireless Pressure Sensor for High-Temperature Applications. Sensors, 2017, 17, 1963.	3.8	21
24	AlN-Based Ceramic Patch Antenna-Type Wireless Passive High-Temperature Sensor. Micromachines, 2017, 8, 301.	2.9	19
25	Acetone Sensing Properties of a Gas Sensor Composed of Carbon Nanotubes Doped With Iron Oxide Nanopowder. Sensors, 2015, 15, 28502-28512.	3.8	18
26	High-Performance MIM Capacitors for a Secondary Power Supply Application. Micromachines, 2018, 9, 69.	2.9	18
27	A Novel Temperature and Pressure Measuring Scheme Based on LC Sensor for Ultra-High Temperature Environment. IEEE Access, 2019, 7, 162747-162755.	4.2	18
28	A Wireless Passive LC Resonant Sensor Based on LTCC under High-Temperature/Pressure Environments. Sensors, 2015, 15, 16729-16739.	3.8	17
29	A Room-Temperature CNT/Fe3O4 Based Passive Wireless Gas Sensor. Sensors, 2018, 18, 3542.	3.8	17
30	A High-Performance LC Wireless Passive Pressure Sensor Fabricated Using Low-Temperature Co-Fired Ceramic (LTCC) Technology. Sensors, 2014, 14, 23337-23347.	3.8	16
31	Temperature and Pressure Composite Measurement System Based on Wireless Passive <i>LC</i> Sensor. IEEE Transactions on Instrumentation and Measurement, 2021, 70, 1-11.	4.7	16
32	A Wide-Range Displacement Sensor Based on Plastic Fiber Macro-Bend Coupling. Sensors, 2017, 17, 196.	3.8	15
33	Substrate Integrated Waveguide (SIW)-Based Wireless Temperature Sensor for Harsh Environments. Sensors, 2018, 18, 1406.	3.8	15
34	Tunable Plasmon-Induced Transparency with Ultra-Broadband in Dirac Semimetal Metamaterials. Plasmonics, 2019, 14, 1717-1723.	3.4	14
35	MWCNTs/WS2 nanocomposite sensor realized by LC wireless method for humidity monitoring. Sensors and Actuators A: Physical, 2019, 290, 207-214.	4.1	14
36	Phase Interrogation Used for a Wireless Passive Pressure Sensor in an 800 °C High-Temperature Environment. Sensors, 2015, 15, 2548-2564.	3.8	13

#	Article	IF	CITATIONS
37	MgO Single Crystals MEMS-Based Fiber-Optic Fabry–Perot Pressure Sensor for Harsh Monitoring. IEEE Sensors Journal, 2021, 21, 4272-4279.	4.7	13
38	Measurement of relative permittivity of LTCC ceramic at different temperatures. AIP Advances, 2014, 4, .	1.3	12
39	Al2O3-Based a-IGZO Schottky Diodes for Temperature Sensing. Sensors, 2019, 19, 224.	3.8	12
40	High Performance Amorphous IGZO Thin-Film Transistor Based on Alumina Ceramic. IEEE Access, 2019, 7, 184312-184319.	4.2	12
41	An Insertable Passive LC Pressure Sensor Based on an Alumina Ceramic for In Situ Pressure Sensing in High-Temperature Environments. Sensors, 2015, 15, 21844-21856.	3.8	11
42	Wireless passive separated LC temperature sensor based on high-temperature co-fired ceramic operating up to 1500 ŰC. Journal of Micromechanics and Microengineering, 2019, 29, 035015.	2.6	11
43	A MoS2 Nanoflakes-Based LC Wireless Passive Humidity Sensor. Sensors, 2018, 18, 4466.	3.8	10
44	Hydrophilic Direct Bonding of MgO/MgO for High-Temperature MEMS Devices. IEEE Access, 2020, 8, 67242-67249.	4.2	10
45	Design and Fabrication of a Thick Film Heat Flux Sensor for Ultra-High Temperature Environment. IEEE Access, 2019, 7, 180771-180778.	4.2	9
46	Surface characterization of patterning on MgO single crystals using wet chemical etching process to advance MEMS devices. Journal of Micromechanics and Microengineering, 2020, 30, 015001.	2.6	9
47	Fabrication of micro-trench structures with high aspect ratio based on DRIE process for MEMS device applications. Microsystem Technologies, 2013, 19, 1097-1103.	2.0	8
48	Glass-SOI-Based Hybrid-Bonded Capacitive Micromachined Ultrasonic Transducer With Hermetic Cavities for Immersion Applications. Journal of Microelectromechanical Systems, 2016, 25, 976-986.	2.5	8
49	Dual-wavelength demodulation technique for interrogating a shortest cavity in multi-cavity fiber-optic Fabry–Pérot sensors. Optics Express, 2021, 29, 32658.	3.4	8
50	A Wireless Passive Vibration Sensor Based on High-Temperature Ceramic for Harsh Environment. Journal of Sensors, 2021, 2021, 1-9.	1.1	7
51	Accurate Real-Time Temperature Measurement Method in Ultra-High Temperature Rotational Environments for Aero Engines/Turbines. IEEE Sensors Journal, 2022, 22, 6482-6490.	4.7	7
52	A Passive Pressure Sensor Fabricated by Post-Fire Metallization on Zirconia Ceramic for High-Temperature Applications. Micromachines, 2014, 5, 814-824.	2.9	6
53	A MEMS Fiber-Optic Fabry-Perot Vibration Sensor for High-Temperature Applications. IEEE Access, 2022, 10, 42908-42915.	4.2	6
54	A novel readout system for wireless passive pressure sensors. Photonic Sensors, 2014, 4, 70-76.	5.0	5

#	Article	IF	CITATIONS
55	Microwave Wire Interrogation Method Mapping Pressure under High Temperatures. Micromachines, 2018, 9, 11.	2.9	5
56	A Novel Capacitive Microwave Power Sensor Based on Double MEMS Cantilever Beams. IEEE Sensors Journal, 2022, 22, 11803-11809.	4.7	5
57	Investigation of the onset voltage for the design of a microfabricated colloid thruster. IEEE/ASME Transactions on Mechatronics, 2006, 11, 66-74.	5.8	3
58	Integration of GaAs/In _{0.1} Ga _{0.9} As/AlAs resonance tunneling heterostructures into microâ€electroâ€mechanical systems for sensor applications. Physica Status Solidi (A) Applications and Materials Science, 2010, 207, 462-467.	1.8	3
59	The Effect of Drain/Gate Bias on Electromechanical Coupling Effect in Accelerometer Based on MESFET. IEEE Sensors Journal, 2011, 11, 384-388.	4.7	3
60	Liquid level sensor based on CMFTIR effect in polymer optical fiber. Photonic Sensors, 2016, 6, 312-317.	5.0	3
61	A Novel Ceramic-Based Heat Flux Sensor Applied for Harsh Heat Flux Measurement. , 2018, , .		3
62	Capacitive Pressure Sensor With Integrated Signal-Conversion Circuit for High-Temperature Applications. IEEE Access, 2020, 8, 212787-212793.	4.2	3
63	A Ceramic Diffusion Bonding Method for Passive LC High-Temperature Pressure Sensor. Sensors, 2018, 18, 2676.	3.8	2
64	A Differential Split-Type Pressure Sensor for High-Temperature Applications. IEEE Access, 2021, 9, 20641-20647.	4.2	2
65	An optimized pulse coupled neural network image de-noising method for a field-programmable gate array based polarization camera. Review of Scientific Instruments, 2021, 92, 113703.	1.3	2
66	A 4-Channel High-Precision Real-Time Pressure Test System for Irregularly Variable High Temperature Environments. IEEE Sensors Journal, 2022, 22, 8104-8112.	4.7	2
67	å^©ç""微机电系统技æœ⁻å^¶ä½œå¼⁻曲结构è¡ïé¢ æ—çº¿æ—æºæŸ"性åŠé€Ÿåº¦è®¡. Frontiers o	ี In£ œrmati	orzTechnolo
68	Time Synchronization Algorithm for the Skiing Monitoring System. IEEE Transactions on Instrumentation and Measurement, 2022, 71, 1-9.	4.7	2
69	A Cantilever Accelerometer Based on Resonant Tunneling Diode. , 2007, , .		1
70	Piezoresistive properties of resonant tunneling diodes. Frontiers of Electrical and Electronic Engineering in China: Selected Publications From Chinese Universities, 2007, 2, 449-453.	0.6	1
71	Piezoresistivity in GaAs/In _{<i>x</i>} Ga _{1–<i>x</i>} As/AlAs superlattice structures. Physica Status Solidi - Rapid Research Letters, 2008, 2, 43-45.	2.4	1

72 Design of T-shape vector hydrophone based on MEMS. , 2011, , .

1

#	Article	IF	CITATIONS
73	Microâ€electroâ€mechanical systems capacitive ultrasonic transducer with a higher electromechanical coupling coefficient. Micro and Nano Letters, 2015, 10, 541-544.	1.3	1
74	Synchronous Online Monitoring of Rotational Speed and Temperature for Rotating Parts in High Temperature Environment. IEEE Access, 2021, 9, 96257-96266.	4.2	1
75	An LC Wireless Passive Pressure Sensor Based on Single-Crystal MgO MEMS Processing Technique for High Temperature Applications. Sensors, 2021, 21, 6602.	3.8	1
76	Manufacturing a langasite crystal microstructure for a high-temperature environment. Vacuum, 2022, , 111252.	3.5	1
77	Package improvements and testing of a novel MEMS bionic vector hydrophone. , 2010, , .		0
78	Studies of the electromechanical coupling characteristics based on cantilever-mass. , 2011, , .		0
79	Measurement of piezoresistance coefficient with different gate voltages of GaN HEMT micro-accelerometer. , 2011, , .		0
80	Embedded seal cavity preparation technology based on the zirconia. , 2013, , .		0
81	Design and measurement of MEMS capacitive ultrasonic transducer. , 2015, , .		0
82	Passive wireless pressure sensor fabricated in low-temperature co-fired ceramic technology. Proceedings of the Institution of Mechanical Engineers, Part N: Journal of Nanoengineering and Nanosystems, 2015, 229, 160-165.	0.1	0
83	Systematic Theoretical Analysis of Dual-Parameters RF Readout by a Novel LC-Type Passive Sensor. Modelling and Simulation in Engineering, 2017, 2017, 1-11.	0.7	0
84	Research on 355 nm all-solid-state ultraviolet laser processing through silicon holes. Journal of Laser Applications, 2019, 31, 022003.	1.7	0
85	Interface Characterization and Analysis of 4H-SiC Direct Bonding Structure Based on Plasma Processing. ECS Journal of Solid State Science and Technology, 2021, 10, 034003.	1.8	0